Interference Modeling and Capacity Analysis for Microfluidic Molecular Communication Channels

A. Ozan Bicen, *Student Member, IEEE*, and Ian F. Akyildiz, *Fellow, IEEE*

Abstract—The impact of the interference on the molecular communication (MC) between a transmitter and receiver pair which are connected through a microfluidic channel containing fluid flow is investigated. The interference modeling and the capacity analysis is performed based on the microfluidic channel geometry, the flow velocity, and the distance. During the analysis, time-scale of biological oscillators is specifically targeted, which is in the range of several minutes to a few hours. The signal-to-interference and noise ratio is shown to be constant with respect to the location of the interfering transmitter. The capacity of the MC link between the designated transmitter and the corresponding receiver is shown to be upper bounded by 1 bit/per channel use when exposed to a single interfering transmitter. For the multiple, i.e., N, transmitters, the decay of pairwise MC capacity is also studied as a factor of N. Finally, placement of the two transmitter and receiver pairs on the opposite sides of the microfluidic channel is studied. Three different microfluidic interference channel configurations, i.e., both-sided interference (microfluidic X channel), one-sided interference (microfluidic Z channel), and interference-free, are proposed based on the distance of the receiver from the interfering transmitter, microfluidic channel cross section, and the fluid flow velocity. For large-scale integration of chemical analysis systems on a microfluidic chip, the provided information-theoretic analysis and the capacity expressions for the MIC can be utilized to analyze the throughput of the chip, which can lead to improvement in efficiency and optimization of the design.

Index Terms—Capacity analysis, interference avoidance, interference modeling, microfluidics, molecular communication (mc).

I. INTRODUCTION

SPECTACULAR evolution of the microfluidic chip technologies has enabled miniaturization, parallelization, automation, and integration of chemical assays for detection, separation, reaction, and sample manipulation operations. Currently, microfluidic platforms for chemical analysis systems are planned to enable rapid and cost-efficient processing of the application-specific distinct molecules with low reagent consumption [1]–[5]. These advances in the microfluidic chip technologies and their salient features for entirely molecular sensing and computation have further entailed the networking of distinct microfluidic systems, i.e., *lab on a chip* [6]–[8]. For this purpose, the emerging field of molecular communication

(MC), in which the molecular concentration signals are modulated to carry information, stands as a promising solution to enable information transfer among distinct chemical systems [9], [10]. Consequently, molecular nanonetworks are emerging as the convergence of the large-scale integration of microfluidic systems and MC over microfluidic channels with the objective of *high throughput*, *multi-step* on chip chemical automation in a microfluidic platform.

Molecular nanonetworks can facilitate not only higher throughput and accuracy, but also the automation of biochemical assays that would otherwise require the intervention of an external human operator. In this respect, the distinct patches of chambers can be connected through microfluidic channels to develop bacteria-based chemical analysis systems [11], [12]. Bacteria are highly capable of detecting biomolecules [13]–[19]. Furthermore, bacteria can be genetically engineered to function as a biological molecular oscillator, so that, they can be utilized as the transmitter and receiver nodes for MC in a microfluidic platform [12], [20]–[22]. Therefore, bacteria-based molecular nanonetworks can be utilized in microfluidic platforms to enable integrated assay operations in multiple steps via on-chip information transfer. Using bacteria as the *chemist* inside microfluidic platform, MC between bacteria populations can combine multi-stage reactions on a single microfluidic chip.

A typical point-to-point MC architecture on a microfluidic chip is illustrated in Fig. 1. In this architecture, the transmitter and receiver chambers, where the transmitter and the receiver nodes can be hosted, respectively, are connected over a microfluidic channel with fluid flow. In response to a specific stimulus, e.g., external molecular input, the transmitter node releases a concentration of molecules, i.e., transmits the information carrying molecular signal, which propagates through the transmitter chamber, the microfluidic channel, and the receiver chamber via diffusion, convection, and diffusion again, respectively, until reaching to the receiver node.

Towards enabling the parallel molecular processing and computation on a chip, the microfluidic channels can also be used to connect multiple transmitter and receiver pairs. The microfluidic MC channel, can empower parallel testing, processing, and preparation of the chemical samples on a microfluidic chip. In the multi-pair MC communication system, we consider that each transmitter is aimed to communicate using same type of molecules with only its designated receiver. However, the transmissions of multiple transmitters using same type of molecules yield interference to each other. The interference effect coupled with the physical limitations of microfluidic channels call for a thorough analysis and efficient design of MC schemes to realize nano communications in microfluidic platforms. The research on the information-theoretic study of
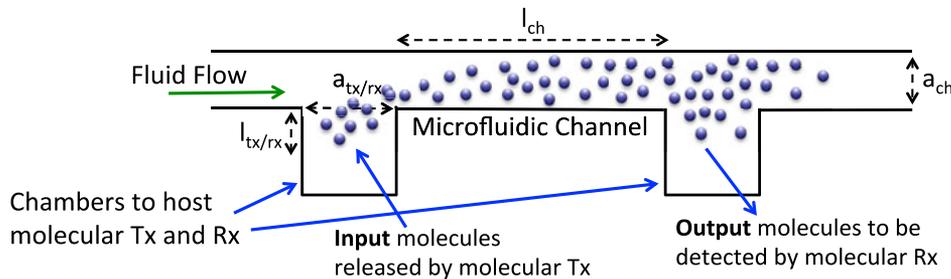
Fig. 1. The conceptual illustration of the microfluidic channel with transmitter and receiver chambers. $l_{\rm ch}$ is the microfluidic channel distance between the transmitter and the receiver, $a_{\rm ch}$ is the height of the microfluidic channel, $l_{\rm tx/rx}$ is the distance from the molecular transmitter to the microfluidic channel (the distance from the microfluidic channel to the molecular receiver), and $a_{\rm tx/rx}$ is the chamber width.

the MC has been a research field of interest recently [24]–[27]. So far, to the best of our knowledge, there is no prior work on analytical modeling of interference and capacity analysis for microfluidic channels from the MC point of view.

In [28], for the MC based on free-space diffusion, modeling of interference is performed for multiple transmitting nanomachines. The transmitters are taken to be spatial Poisson distributed, and the statistics of the received signal is studied. The provided analysis aims to characterize the interference in free-space MC under random distribution of transmitters, which is not applicable to microfluidic MC channels. In [24], the information capacity of a free-space MC system is investigated. The capacity is expressed based on the diffusion constant, the distance between the transmitter and the receiver, and the bandwidth of the transmitted signal. Additionally, the thermodynamic power spent at the transmitter for molecule emission is used for capacity evaluation. The capacity formulation for MC is applicable only for a single molecular transmitter and receiver pair, and for purposes of solely diffusion-based molecular propagation. In [25], the information capacity in a molecular nanonetwork is investigated based on stochastic models in chemically reacting systems. The free-space MC models for a transmitter and receiver pair, single transmitter and multiple receivers, and multiple transmitters and single receiver scenarios are also proposed. For each of these models, the capacity expressions are derived for molecular transport solely based on diffusion. However, the capacity analyses in [24] and [25] do not capture the attenuation, and the noise characteristics of the flow-induced molecular transport and are not suitable for the MC over microfluidic channels.

In this work, based on the channel modeling and the noise analysis performed in [29] and [30], respectively, we investigate the interference effects and the capacity of the microfluidic MC channel, i.e., microfluidic interference channel (MIC). The interference amplitude and variance, and the interference-induced noise at the receiver are modeled first. In the course of this work, we focus on the received signal level and do not assume any underlying encoding and modulation schemes. Then, the MC link capacity under interference is studied for the single interfering transmitter and the multiple interfering transmitter cases. The impact of the distance as well as the number of interfering transmitters are investigated. The microfluidic MC channel capacity is shown to be severely constrained under the interference, which requires the development of practical detection schemes by con-

sidering capabilities of the biological molecular receivers, e.g., genetically engineered bacteria, to distinguish the transmission of designated transmitter from interferer signals.

Furthermore, the placement of the chambers on the opposite sides of the microfluidic channel is also investigated for two pairs of transmitters and receivers. Each transmitter communicates with its designated receiver on the same side of the microfluidic channel, and causes interference to the undesignated receiver on the opposite side based on the flow velocity and the microfluidic channel configuration. Accordingly, three microfluidic channel configurations are presented based on the distance of the receiver from the interfering transmitter, microfluidic channel cross-section and the fluid flow: 1) microfluidic X channel, i.e., both receivers are exposed to interference, 2) microfluidic Z channel, i.e., only one of the receivers is exposed to the interference, and 3) microfluidic interference-free channel, i.e., none of the receivers is exposed to interference. The provided analysis for capacity, enables information-theoretic evaluation of the microfluidic MC systems. The throughput and the accuracy of these systems can be assessed via the information theory.

The remainder of this paper is organized as follows. In Section II, we provide the system model for the MC over microfluidic channels. In Section III, we model the interference in the microfluidic channels. In Section IV, capacity of the microfluidic MC channel under interference is investigated. In Section V, MIC configurations are presented. We provide concluding remarks in Section VI.

II. MICROFLUIDIC MC CHANNEL

In this section, we present the system model for the microfluidic MC channel which forms the basis for interference modeling and capacity analysis. The microfluidic channel and chamber dimensions are illustrated in Fig. 1. The molecular transmitter and the receiver are placed in the chambers which are attached to a connecting microfluidic channel with fluid flow. It can be inferred from [30] that the microfluidic MC channel can be reasonably modeled as a linear communication channel, and the memoryless AWGN model of a microfluidic MC system can be developed when the range of frequencies for a molecular signal is limited to a few millihertz (mHz), which conforms with the capabilities of biological oscillators such as genetically engineered bacteria [12], [21]–[23].

The transmitter node modulates the information on the molecular signal x by changing the level, i.e., the amount, of the released molecular concentration. We assume the transmitter nodes are adjusted to change the released concentration level with a rate of $f_0 = 1/T_0$, and T_0 is the period of the signal. Furthermore, we assume the bandwidth of the molecular receiver is greater or equal to f_0, i.e., the molecular receiver is capable of responding to the changes in the received signal level with a frequency of f_0. Therefore, the molecular receiver can respond to the changes in the input signal with frequency f_0 by the transmitter. The transmitted molecular signal x is subject to a variance constraint ϕ^2 for each transmission as

$$\mathrm{E}[x^2] \leq \phi^2. \tag{1}$$

The received molecular signal y is given by

$$y = \alpha x + n \tag{2}$$

where α is the channel gain, and n is AWGN [30]. We provide below the complete channel model for the MC link between a transmitter and a receiver pair, i.e., point-to-point MC link.

A. Attenuation

The fluid flow is characterized as laminar, steady, unidirectional, and driven by the pressure drop across the microfluidic channel [31]. For the rectangular cross-section microfluidic channel, the area-averaged flow velocity u_{ch}, which is also the propagation velocity through the microfluidic channel, is given by [32]

$$u_{ch} = \frac{a_{ch}^2}{12\mu l_{ch}} \left(1 - 0.63 \frac{a_{ch}}{b_{ch}} \right) \Delta p \tag{3}$$

where μ is the viscosity of the fluid, l_{ch} is the microfluidic channel length, a_{ch} is the microfluidic channel height, b_{ch} is the microfluidic channel width, and Δp is the pressure drop across the microfluidic channel. Molecular transport via the fluid flow is modeled via the one-dimensional solution of the convection-diffusion equation for the microfluidic channel [33]–[37].

In this work, we use the temporal frequency f for analysis, apart from our former works based on spatial frequency ν, i.e., in radians $k = 2\pi\nu$ [29], [30]. The equality of both representations for molecular propagation is presented in [29]. The conversion is provided by [29]

$$f = \frac{k}{2\pi u} \tag{4}$$

where u is the propagation velocity in the medium. While the spatial frequency provides compact representation for formulations, the temporal frequency is preferred during the course of this work to relate our results to time-scale and the operating frequency of the molecular transmitters and receivers.

The block diagram representation of signal propagation between the transmitter and the receiver pair is given in Fig. 2. We take the transmitter and the receiver chambers identical, i.e., the gains of the transmitter and the receiver chambers are equal. The end-to-end channel gain α is defined as

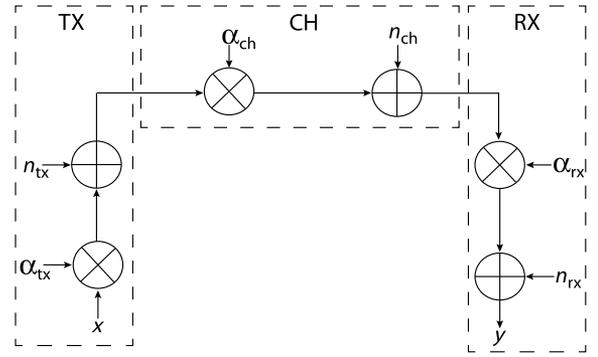$$\alpha = \alpha_{ch} \alpha_{tx/rx}^2 \tag{5}$$

Fig. 2. Block diagram representation of the microfluidic AWGN channel.

where α_{ch} is the gain of the microfluidic channel, $\alpha_{tx/rx}$ is the gain of the transmitter and the receiver chambers. Both chambers have equal gain, i.e., $\alpha_{tx/rx} = \alpha_{tx} = \alpha_{rx}$, since the transmitter and chambers are taken to be identical. For the microfluidic channel, the signal gain is given in [30] based on the obtained impulse response for the microfluidic channel with the laminar flow in [29]. Here, we assume the microfluidic channel is straight, and hence, the signal gain α_{ch} in [30] reduces to

$$\alpha_{ch} = \exp\left(-\frac{4\pi^2 f_0^2}{u_{ch}^2} D \tau_{ch} \right) \tag{6}$$

where D is the Taylor dispersion adjusted diffusion coefficient for the rectangular microfluidic channels, which is given by [38]

$$D = \left(1 + \frac{8.5 u_{ch}^2 a_{ch}^2 b_{ch}^2}{210 D_0^2 (a_{ch}^2 + 2.4 a_{ch} b_{ch} + b_{ch}^2)} \right) D_0, \tag{7}$$

and τ_{ch} is the propagation delay from the transmitter chamber to the receiver chamber, which is referred as extended microfluidic channel delay in [30] and given by

$$\tau_{ch} = \frac{l_{ch} + a_{tx/rx}}{u_{ch}} \tag{8}$$

where $a_{tx/rx}$ is the width of transmitter and receiver chambers. Both chambers have equal width, i.e., $a_{tx/rx} = a_{tx} = a_{rx}$, since the transmitter and the receiver chambers are taken to be identical, which is illustrated in Fig. 1.

For the identical transmitter and the receiver chambers, the signal gain is obtained as [30]

$$\alpha_{tx/rx} = \exp\left(-\frac{4\pi^2 f_0^2}{u_{tx/rx}^2} D_0 \tau_{tx/rx} \right) \mathrm{sinc}\left(\frac{a_{tx/rx}}{u_{tx/rx}} f_0 \right) \tag{9}$$

where $\tau_{tx/rx}$ and $u_{tx/rx}$ are the propagation delay and the propagation velocity, respectively, at the transmitter and the receiver chambers. Due to the identical dimensions, the propagation delays at the both chambers are equal, i.e., $\tau_{tx/rx} = \tau_{tx} = \tau_{rx}$, which is given by [30]

$$\tau_{tx/rx} = \frac{l_{tx/rx}^2}{2D_0} \tag{10}$$

where $l_{tx/rx}$ is the distance of the transmitter and the receiver placed in the chambers to the microfluidic channel, which is illustrated in Fig. 1. The distances inside the identical chambers
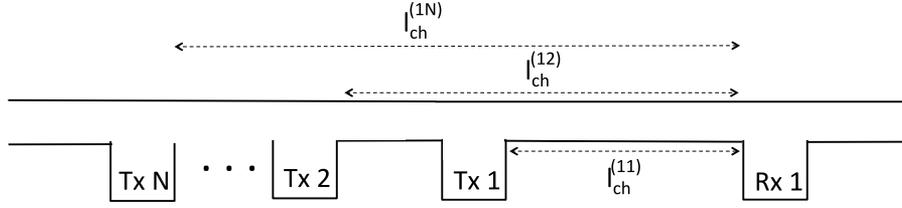
Fig. 3. The illustration of the multiple transmitters (Tx1, Tx 2,..., Tx N), and the receiver (Rx 1) placed on the microfluidic channel. The distances $l_{\text{ch}}^{(11)}$, ..., $l_{\text{ch}}^{(1N)}$ represent the separation between the transmitters and the Rx 1.

are equal for both transmitter and receiver, i.e., $l_{\text{tx/rx}} = l_{\text{tx}} = l_{\text{rx}}$. The propagation velocity at the both chambers are also equal, i.e., $u_{\text{tx/rx}} = u_{\text{tx}} = u_{\text{rx}}$, which is obtained using (10) as

$$u_{\text{tx/rx}} = \frac{l_{\text{tx/rx}}}{\tau_{\text{tx/rx}}}$$

$$= \frac{2D_0}{l_{\text{tx/rx}}}. \qquad (11)$$

The received signal is said to be under the effect of memory when the molecular signal period is less than the propagation duration of the signal through the microfluidic channel, i.e., the following condition is satisfied [30]

$$\frac{1}{f_0} < \tau_{\text{ch}}. \qquad (12)$$

During this study, we focus on the frequencies in the range of a few mHz based on the capabilities and time-scale of the bacteria-based receivers, which are proposed as the potential nanomachines to test and implement molecular receivers [20]–[22]. Therefore, for the physical system we have, $1 \gg f_0 \tau_{\text{ch}}$, and hence, MC channel can be taken as memoryless.

B. Molecular Noise

For sufficiently small frequencies, i.e., the frequency range of biological oscillators based on the genetically engineered bacteria, spectral density of the received molecular signal is shown to be flat, and hence, the Gaussian distribution assumption is valid for molecular noise [30]. Therefore, the microfluidic MC channel can be treated as an AWGN channel for sufficiently small transmission frequency ranges.

The noise effects on the received signal are illustrated in the block diagram in Fig. 2. The propagation noise n is composed of the transmitter/receiver chamber, and the microfluidic channel noises. The molecular propagation noise is shown to be well-approximated based on microfluidic channel noise in [30]. The variance of the microfluidic channel noise σ^2 of the n is derived in [30] as

$$\sigma^2 = \left(2\alpha_{\text{tx/rx}}^4 \frac{D\tau_{\text{ch}}}{u_{\text{ch}}^2} + 4\frac{D_0\tau_{\text{tx/rx}}}{u_{\text{tx/rx}}^2}\alpha_{\text{ch}}^2\alpha_{\text{tx/rx}}^2 \right) 4\pi^2 f_0^2 \phi^2. \qquad (13)$$

The distribution of propagation noise n is taken as

$$n \sim \mathcal{N}\left(0, \sigma^2\right). \qquad (14)$$

Next, we model the interference in microfluidic channels before proceeding to the capacity analysis.

III. INTERFERENCE IN MICROFLUIDIC MC CHANNEL

Each transmitter attempts to communicate with the receiver, meanwhile causing interference to other transmitters' signal at the receiver, which is illustrated in Fig. 3. We assume there is no coordination among the transmitters.

We characterize the interference based on the received signal rather than assuming employed modulation and coding techniques. The interference effect is modeled based on the flow velocity, channel dimensions, and the distance between the transmitters and the receiver. In the following sections, we present an analytic model for the interference magnitude and interference-induced noise.

A. Interference Magnitude and Variance at the Receiver

For the interference modeling, we assume that all chambers are identical. The channel gain α_{ij} for the interfering signal from transmitter j at the receiver i is obtained based on (5) as

$$\alpha_{ij} = \alpha_{\text{ch}}^{(ij)}\alpha_{\text{tx/rx}}^2 \qquad (15)$$

where $\alpha_{\text{tx/rx}}$ is given in (9), and $\alpha_{\text{ch}}^{(ij)}$ is the microfluidic channel gain between the transmitter j and the receiver i, which is given based on (6) as

$$\alpha_{\text{ch}}^{(ij)} = \exp\left(-\frac{4\pi^2 f_0^2}{u_{\text{ch}}^2}D\tau_{\text{ch}}^{(ij)}\right) \qquad (16)$$

where $\tau_{\text{ch}}^{(ij)}$ is the delay between the transmitter j and receiver i, which is given based on the distance $l_{\text{ch}}^{(ij)}$ between interferer chamber j and the receiver chamber i using (8) as

$$\tau_{\text{ch}}^{(ij)} = \frac{l_{\text{ch}}^{(ij)}}{u_{\text{ch}}}. \qquad (17)$$

The variance ζ_{ij}^2 of the interference from interferer j at the receiver i is defined to incorporate the interference at the receiver i as

$$\zeta_{ij}^2 = (\alpha_{\text{ch}}^{(ij)})^2\alpha_{\text{tx/rx}}^4\phi_j^2 \qquad (18)$$

where ϕ_j^2 is the interferer signal variance. Furthermore, the memory condition given in (12) also does not hold for interferer signals, i.e.,

$$\frac{1}{f_0} \gg \tau_{\text{ch}}^{(ij)}. \qquad (19)$$

Therefore, all transmissions in the MIC are memoryless. Next, we analyze the interference-induced noise of the MIC link

using the performed modeling for interference magnitude here.

B. Interference-Induced Molecular Noise

In MIC, the receiver i is also exposed to the interference-induced noise n_{ij} from transmitter j. The noise in the microfluidic channel is shown to be dominating the noise in the chambers [30]. The interference-induced noise variance ξ_{ij}^2 at the receiver i due to the interference caused by transmitter j can be obtained based on the attenuation in the microfluidic channel as

$$\xi_{ij}^2 = (1 - (\alpha_{\text{ch}}^{(ij)})^2)\alpha_{\text{tx/rx}}^4 \phi_j^2. \tag{20}$$

For the frequency range of interest, i.e., a few mHz, the molecular noise is shown to be taken distributed as white Gaussian [30]. Thus, the distribution interference-induced noise n_{ij} is given by

$$n_{ij} \sim \mathcal{N}\left(0, \xi_{ij}^2\right). \tag{21}$$

C. Multiple Transmitters

Due to received signal from multiple transmitters, we assume that the molecular receiver is capable of detecting and producing a distinct response for multiple levels of received concentration signal. Furthermore, the largest distance between transmitters and the receiver, i.e., the distance between Tx N and the RX in Fig. 3, is sufficiently small, i.e.,

$$T_0 \gg \frac{l_{\text{ch}}^{(1N)} + a_{\text{tx/rx}}}{u_{\text{ch}}}, \tag{22}$$

that all signals can be taken as received all together, and then, a total response is produced by the molecular receiver. Moreover, the difference in transmission instants of multiple transmitters is negligible due to low rate of change in the signal level f_0, i.e., large signal period T_0 compared to the total propagation delay as stated in (22).

IV. CAPACITY ANALYSIS

In this section, we analyze the capacity of the microfluidic MC channel under the interference from single and multiple interferer transmitter cases. The signal-to-interference and noise ratio (SINR) and capacity expressions are derived for the MIC, and the impact of physical parameters is elaborated.

A. Single Interferer

Here, we assume there are two transmitters that are attached to the microfluidic channel, i.e., Tx 1 and Tx 2 in Fig. 3. The transmitters cause interference to each other at the receiver. We focus on the individual MC capacity of the transmitters with a receiver connected to the microfluidic channel, i.e., RX in Fig. 3. Therefore, the impact of the interference from a single interferer transmission on the MIC capacity is investigated.

1) SINR: The variance of the received signal at the receiver i under the interference is given by

$$\psi_i^2 = \alpha_i^2 \phi_i^2 + \sigma_i^2 + \zeta_{ij}^2 + \xi_{ij}^2 \tag{23}$$

where α_i and ϕ_i^2 represent the channel gain and the variance of the transmitted molecular signal, respectively; ζ_{ij}^2 represent the

variance of the interference component in the received signal caused by the interferer j at the receiver i; σ_i^2 is the variance of the molecular propagation noise at receiver i; ξ_{ij}^2 represents the variance of the interference-induced noise in the received signal caused by the interferer j at the receiver i. The computation of α_i, σ_i^2, ζ_{ij}^2, and ξ_{ij}^2 are given in (5), (13), (18) and (20), respectively. Overall, the noise distribution for MIC is given by

$$n_i \sim n_{ii} + n_{ij}$$
$$\sim \mathcal{N}\left(0, \sigma_i^2 + \xi_{ij}^2\right). \tag{24}$$

SINR at receiver i under interference from interferer j is obtained as

$$\text{SINR}_i = \frac{\psi_i^2}{\sigma_i^2 + \zeta_{ij}^2 + \xi_{ij}^2}. \tag{25}$$

2) Capacity: In our analysis, we look at the frequencies in the range of few mHz such that MC channel can be taken as linear [30]. We further assume that the transmitted signal is drawn from a Gaussian distribution. Accordingly, we utilize the AWGN channel capacity as the basis of our analysis.

The mutual information among the transmitter i and the receiver i under the interference from transmitter j can be found via definition of the mutual information and the entropy of a Gaussian random variable given in [39] as

$$I(x_i; y) = \frac{1}{2} \log_2\left(2\pi e\left(\alpha_{ii}^2 \phi_i^2 + \zeta_{ij}^2 + \sigma_i^2 + \xi_{ij}^2\right)\right)$$
$$- \frac{1}{2} \log_2\left(2\pi e\left(\zeta_{ii}^2 + \zeta_{ij}^2 + \sigma_i^2 + \xi_{ij}^2\right)\right)$$
$$= \frac{1}{2} \log_2\left(1 + \frac{\alpha_{ii}^2 \phi_i^2}{\zeta_{ij}^2 + \sigma_i^2 + \xi_{ij}^2}\right) \text{ bits per channel use.} \tag{26}$$

Based on the fact that transmitter changes the transmitted signal level with an interval of $1/f_0$, i.e., degrees of freedom per second is f_0, which can also be perceived as the channel use duration, so the capacity is

$$C_i = \frac{1}{T_0} \log_2\left(1 + \frac{\alpha_i^2 \phi_i^2}{\sigma_i^2 + \zeta_{ij}^2 + \xi_{ij}^2}\right) \text{ bits/s.} \tag{27}$$

Under the assumption that the variance of the transmitted signals from both transmitters are equal, i.e., $\phi_i^2 = \phi_j^2$, the capacity of the MC link between the designated transmitter i and the receiver i under a single interferer j can be obtained based on the physical system parameters as

$$C_i = \frac{1}{T_0} \log_2\left(1 + \alpha_i^2 \middle/ \left(+ \left(2\alpha_{\text{tx/rx}}^4 \frac{D\tau_{\text{ch}}^{(ii)}}{u_{\text{ch}}^2}\right.\right.\right.$$
$$+ 4\frac{D\tau_{\text{tx/rx}}}{u_{\text{tx/rx}}^2}(\alpha_{\text{ch}}^{(ii)})^2 \alpha_{\text{tx/rx}}^2\right)4\pi^2 \frac{1}{T_0^2}$$
$$\left.\left.+ \alpha_{ij}^2 + (1 - (\alpha_{\text{ch}}^{(ij)})^2)\alpha_{\text{tx/rx}}^4 \phi_j^2\right)\right) \text{ bits/s.} \tag{28}$$
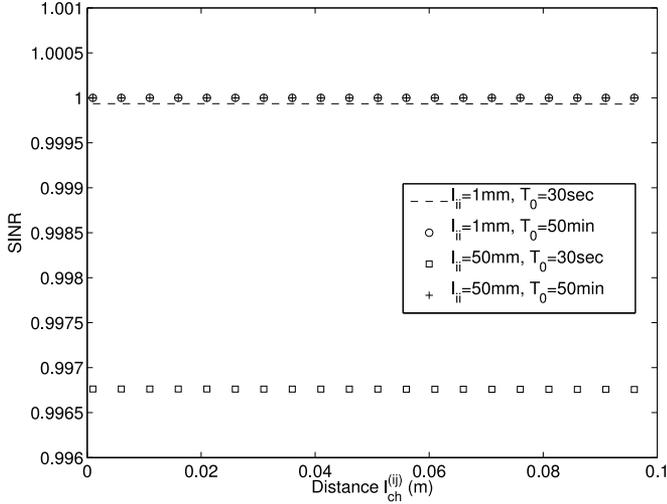
Fig. 4. SINR with respect to the interferer distance $l_{\text{ch}}^{(ij)}$.
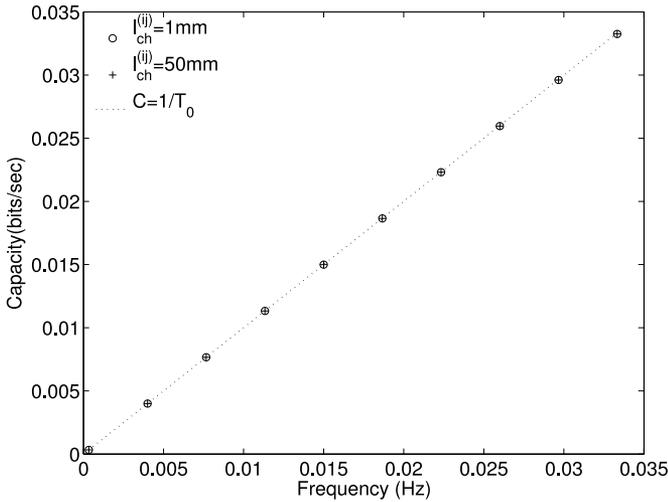

Fig. 5. Capacity with respect to the frequency $f_0 = 1/T_0$.

TABLE I
THE VALUES OF THE PHYSICAL PARAMETERS

Parameter	Value
D_0 (Diffusion constant)	$10^{-9}\,\text{m}^2/\text{s}$
a_{ch} (microfluidic channel width)	$250\,\mu\text{m}$
b_{ch} (microfluidic channel height)	$10\,\mu\text{m}$
$a_{\text{tx/rx}}$ (chamber width)	$150\,\mu\text{m}$
$l_{\text{tx/rx}}$ (chamber length)	$1\,\mu\text{m}$
u_{ch} (flow velocity)	$10^{-2}\,\text{m/s}$

The SINR and the capacity for the single interferer case are studied numerically in Figs. 4 and 5, respectively. For the evaluations, the parameter values given in Table I are used. We characterize the SINR and the capacity with respect to the distance $l_{\text{ch}}^{(ij)}$ between the interfering transmitter j and the designated receiver i. The distance $l_{\text{ch}}^{(ii)}$ between the designated transmitter

i and the designated receiver i is evaluated at 1 and 50 mm. The period T_0 of the receiver is evaluated at 30 s and 50 min.

In Fig. 4, the SINR at the receiver i is presented with respect to the distance of the interferer transmitter. The SINR curves are shown to be upper bounded by 1 and stay constant for various T_0 and $l_{\text{ch}}^{(ii)}$ pairs. In Fig. 5, we study of the capacity under a single interferer with respect to f_0. Since the SINR is constant and almost equal to 1, capacity is shown to be linearly scaling with the reciprocal of the channel use duration. Additionally, it should be noted that the channel capacity curves in Fig. 5 overlaps for different $l_{\text{ch}}^{(ij)}$ values due to negligible change in the SINR.

B. Multiple Interferers

Here, we assume there are multiple transmitters that are attached to the microfluidic channel, i.e., Tx 1 to Tx N in Fig. 3. The impact of interference from multiple interferers on the MC capacity of a single transmitter and receiver pair is studied.

1) SINR: Under multiple interferers, the variance of the received signal at the receiver i is given by

$$\psi_i^2 = \alpha_i^2 \phi_i^2 + \sigma_i^2 + \sum_{j=2}^{N} \zeta_{ij}^2 + \xi_{ij}^2 \qquad (29)$$

where N is the number of transmitters. We take Tx 1 as the designated transmitter with $N-1$ remaining interferers. Overall, the noise distribution under multiple interferers is given by

$$n_i \sim n_{ii} + \sum_{j=2}^{N} n_{ij}$$

$$\sim \mathcal{N}\left(0, \sigma_i^2 + \sum_{j=2}^{N} \xi_{ij}^2\right). \qquad (30)$$

Accordingly, the SINR at receiver i under interference is obtained as

$$\text{SINR}_i = \frac{\psi_i^2}{\sigma_i^2 + \sum_{j=2}^{N} \zeta_{ij}^2 + \xi_{ij}^2}. \qquad (31)$$

2) Capacity: Similar to single interferer case, based on the AWGN model, the capacity under multiple interferers is obtained as

$$C_i = \frac{1}{T_0} \log_2\left(1 + \frac{\alpha_{ii}^2 \phi_i^2}{\sigma_i^2 + \sum_{j=2}^{N} \zeta_{ij}^2 + \xi_{ij}^2}\right) \text{ bits/s.} \qquad (32)$$

We further extend our analysis over the case where the variances of the input signals from all transmitters are equal in value, i.e., $\phi_i = \phi_j$ for all $i, j \in \{1, \ldots, N\}$. The capacity of the receiver
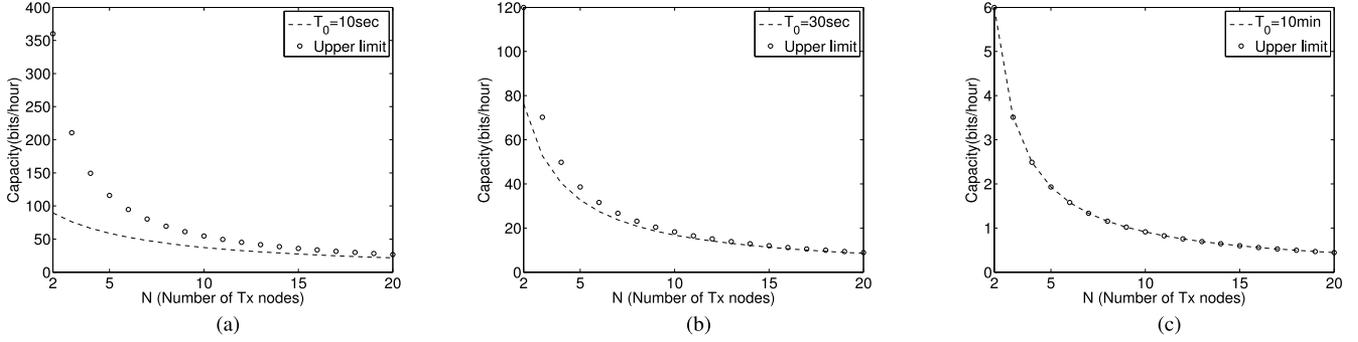
Fig. 6. The capacity under multiple interferers in (32) versus the upper limit in (33) for (a) $T_0 = 10$ s, (b) $T_0 = 30$ s, and (c) $T_0 = 10$ min.
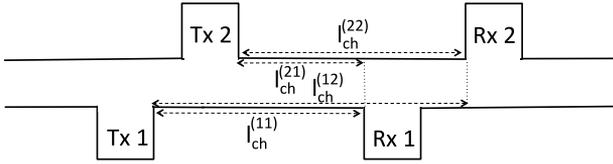

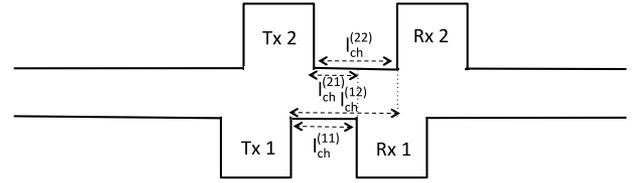Fig. 7. The microfluidic X, i.e., the both-sided interference, channel.
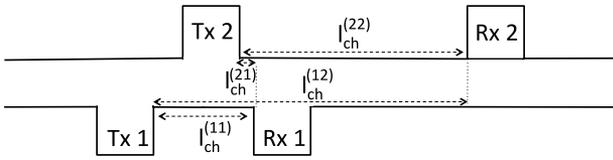

Fig. 8. The microfluidic Z, i.e., the one-sided interference, channel.

Fig. 9. The microfluidic interference-free channel.

Furthermore, similar to single interferer case, capacity scales linearly with reciprocal with the channel use duration.

Numerical results are provided for capacity under multiple interferers in Fig. 6(a)–(c) for $T_0 = 10$ s, $T_0 = 30$ s, and $T_0 = 10$ min, respectively. The values of the physical parameters are listed in Table I, $l_{\text{ch}}^{(11)}$ is set to 50 mm, and the displacement between interfering Tx nodes is taken 0.5 mm. The upper limit on capacity under multiple interferers in (33) is shown to be providing a better approximate of the capacity in (32) as T_0 is increased from 10 s to 10 min. Accordingly, the provided upper limit can be regarded as a good approximation of the MC capacity under interfering transmitters for the frequencies in the range of a few mHz and below, where biological molecular transceivers are expected to operate [23].

V. MIC Configurations

MICs can be realized via various design choices such as utilizing the concentration of distinct type of molecules for communication between different transmitter and receiver pairs, or placing different pairs on distinct microfluidic channels. The use of distinct molecules requires engineering of the specific transmitter and the receiver nodes capable of processing different types of molecular concentrations, meanwhile, the separation of different transmitter and receiver pairs onto distinct microfluidic channels requires larger microfluidic chip size area as well as additional micropumps. Here, we specifically investigate the placement of the two transmitter and receiver pairs on the opposite sides of the microfluidic channel, which use the concentration of same type of molecules for MC.

Each receiver is exposed to the interference from its undesignated transmitter on the opposite side, when its distance to the chamber of the undesignated transmitter is large enough,

i is obtained based on physical system parameters as

$$C_i = \frac{1}{T_0} \log_2 \left(1 + \alpha_{ii}^2 \Big/ \left(\left(2\alpha_{\text{tx/rx}}^4 \frac{D\tau_{\text{ch}}^{(ii)}}{u_{\text{ch}}^2} \right. \right. \right.$$

$$\left. + 4\frac{D\tau_{\text{tx/rx}}}{u_{\text{tx/rx}}^2}(\alpha_{\text{ch}}^{(ii)})^2\alpha_{\text{tx/rx}}^2 \right) 4\pi^2 \frac{1}{T_0^2} + \sum_{j=2}^{N}(\alpha_{\text{ch}}^{(ij)})^2\alpha_{\text{tx/rx}}^4$$

$$\left. \left. + (1 - (\alpha_{\text{ch}}^{(ij)})^2)\alpha_{\text{tx/rx}}^4 \right) \right) = \frac{1}{T_0} \log_2 \left(1 + \alpha_{ii}^2 \Big/ \right.$$

$$\times \left(\left(2\alpha_{\text{tx/rx}}^4 \frac{D\tau_{\text{ch}}^{(ii)}}{u_{\text{ch}}^2} + 4\frac{D\tau_{\text{tx/rx}}}{u_{\text{tx/rx}}^2}(\alpha_{\text{ch}}^{(ii)})^2\alpha_{\text{tx/rx}}^2 \right) 4\pi^2 \frac{1}{T_0^2} \right.$$

$$\left. \left. + (N-1)\alpha_{\text{tx/rx}}^4 \right) \right) \leq \frac{1}{T_0} \log_2 \left(\frac{N}{N-1} \right) \text{ bits/s} \quad (33)$$

where we utilized the fact that attenuation is negligible due to signal period and practical distance values in the range of 1–100 mm, hence, $\alpha_{ii}^2 \approx 1$, $\alpha_{\text{tx/rx}} \approx 1$, and $\left(2\alpha_{\text{tx/rx}}^4 \frac{D\tau_{\text{ch}}^{(ii)}}{u_{\text{ch}}^2} + 4\frac{D\tau_{\text{tx/rx}}}{u_{\text{tx/rx}}^2}(\alpha_{\text{ch}}^{(ii)})^2\alpha_{\text{tx/rx}}^2 \right) 4\pi^2 \frac{1}{T_0^2} \approx 0$.

In (33), it is observed that channel capacity decays from 1 bit/per channel use to 0 as N increases from 2 to infinity.
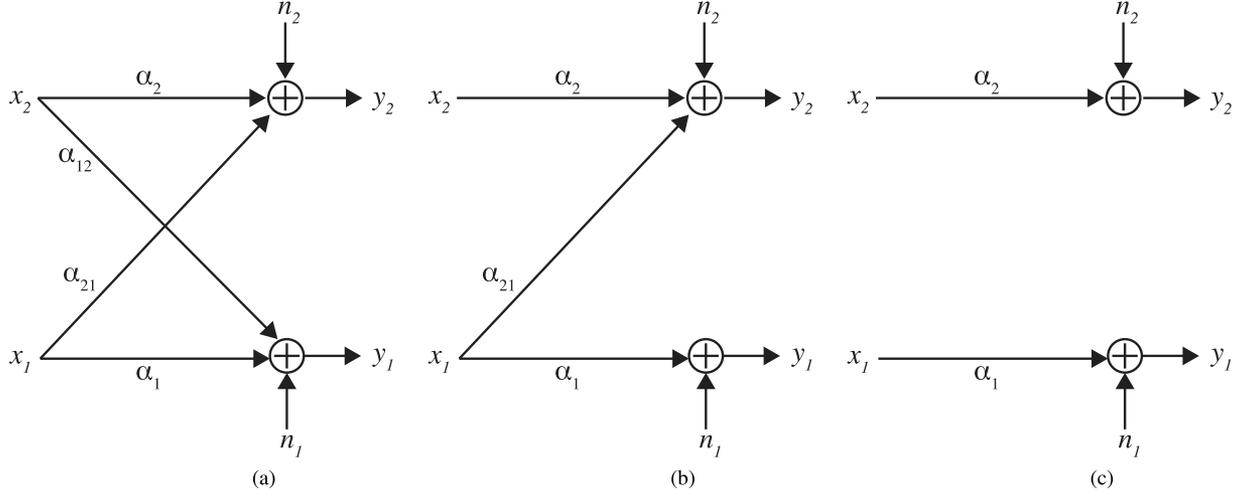
Fig. 10. Block diagram representation of the three MIC configurations: (a) both-sided interference, (b) one-sided interference, (c) and inference-free.

such that the transmitted signal by the undesignated transmitter j can traverse, i.e., diffuse across the microfluidic channel, and reach to the receiver placed at the opposing side. Using the delay expression for the diffusion-based propagation in (10), the condition for the distance between the transmitter j and the receiver i for the interference from the transmitter j at the receiver i is given by

$$l_{ch}^{(ij)} \gg u_{ch}\tau_{int}. \tag{34}$$

where $i \neq j$, and τ_{int} is the needed duration to have the interference by diffusion of the molecules from the one side of the channel to the opposing side, which is obtained via the diffusion delay as

$$\tau_{int} = \frac{a_{ch}^2}{2D_0}. \tag{35}$$

In the following, we describe different MIC configurations based on the distance of the receivers to their corresponding interfering transmitter. Three MIC configurations, namely, the both-sided interference, i.e., the microfluidic X channel, the one-sided interference, i.e., the microfluidic Z channel, and the interference-free configuration are defined.

A. Microfluidic X Channel

In this configuration, both receivers are exposed to the interference from the non-designated transmitter, which is illustrated in Fig. 7. The necessary condition defined in (34) is satisfied for both receivers. The distances between both receivers and their corresponding undesignated transmitters are sufficiently large so that transmitted molecular signal can traverse across the microfluidic channel, i.e.,

$$l_{ch}^{(12)} \gg u_{ch}\tau_{int} \quad \text{and} \quad l_{ch}^{(21)} \gg u_{ch}\tau_{int}. \tag{36}$$

The block diagram representation of the microfluidic X channel is given in Fig. 10(a). The capacity of the MC between the Tx 1

and the Rx 1 is obtained via (28) as

$$C_1 = \frac{1}{T_0} \log_2 \left(1 + \alpha_1^2 \Big/ \left(\left(2\alpha_{tx/rx}^4 \frac{D\tau_{ch}^{(11)}}{u_{ch}^2} \right. \right. \right.$$
$$+ 4\frac{D\tau_{tx/rx}}{u_{tx/rx}^2}(\alpha_{ch}^{(11)})^2\alpha_{tx/rx}^2 \Big) 4\pi^2 \frac{1}{T_0^2}$$
$$\left. \left. + (\alpha_{12}^2 + (1-(\alpha_{ch}^{(12)})^2)\alpha_{tx/rx}^4) \right) \right) \tag{37}$$

and likewise the capacity of the MC between the Tx 2 and the Rx 2 is

$$C_2 = \frac{1}{T_0} \log_2 \left(1 + \alpha_2^2 \Big/ \left(\left(2\alpha_{tx/rx}^4 \frac{D\tau_{ch}^{(22)}}{u_{ch}^2} \right. \right. \right.$$
$$+ 4\frac{D\tau_{tx/rx}}{u_{tx/rx}^2}(\alpha_{ch}^{(22)})^2\alpha_{tx/rx}^2 \Big) 4\pi^2 \frac{1}{T_0^2}$$
$$\left. \left. + (\alpha_{21}^2 + (1-(\alpha_{ch}^{(21)})^2)\alpha_{tx/rx}^4) \right) \right). \tag{38}$$

B. Microfluidic Z Channel

In this configuration, only one of the receivers is exposed to the interference, which is illustrated in Fig. 8. The required condition in (34) for interference holds only for one of the receivers. One of the receivers is placed sufficiently close to its undesignated transmitter such that the molecules released from undesignated transmitter do not travel to the opposing side of the microfluidic channel. Meanwhile the other receiver and its corresponding undesignated transmitter is sufficiently far apart so that the transmitted molecular signal can traverse the microfluidic channel from one side to the other. Thereby, based on Fig. 8 the following conditions are satisfied:

$$l_{ch}^{(12)} \gg u_{ch}\tau_{int} \quad \text{and} \quad l_{ch}^{(21)} \ll u_{ch}\tau_{int}. \tag{39}$$

The block diagram representation of the microfluidic Z channel is presented in Fig. 10(b), where $\alpha_{12} = 0$. In this MIC configuration, the capacity of the MC between the Tx 1 and the Rx 1 is as in (37), while the MC capacity expression for Tx 2 and the Rx 2 in (38) reduces to

$$C_2 = \frac{1}{T_0} \log_2 \left(1 + \alpha_2^2 \Big/ \left(\left(2\alpha_{\text{tx/rx}}^4 \frac{D\tau_{\text{ch}}^{(22)}}{u_{\text{ch}}^2}\right. \right.\right.$$
$$\left.\left.\left. + 4\frac{D\tau_{\text{tx/rx}}}{u_{\text{tx/rx}}^2}(\alpha_{\text{ch}}^{(22)})^2 \alpha_{\text{tx/rx}}^2\right)4\pi^2 \frac{1}{T_0^2}\right)\right). \tag{40}$$

C. Interference-Free Configuration

When both receivers are at a distance to their corresponding undesignated transmitters closer than the required distance for the interference, none of the receivers are exposed to the interference from its non-designated receiver, which is illustrated in Fig. 9. The condition given in (34) does not hold for both receivers, i.e.,

$$l_{\text{ch}}^{(12)} \ll u_{\text{ch}}\tau_{\text{int}} \quad \text{and} \quad l_{\text{ch}}^{(21)} \ll u_{\text{ch}}\tau_{\text{int}}. \tag{41}$$

This placement of the receivers is called the interference-free configuration. The interference-free configuration is illustrated in Fig. 10(c), where $\alpha_{12} = 0$ and where $\alpha_{21} = 0$. In this MIC configuration, the capacity of the MC between the Tx 1 and the Rx 1 is as in (40), while the MC capacity expression for Tx 1 and the Rx 1 in (37) reduces to

$$C_1 = \frac{1}{T_0} \log_2 \left(1 + \alpha_1^2 \Big/ \left(\left(2\alpha_{\text{tx/rx}}^4 \frac{D\tau_{\text{ch}}^{(11)}}{u_{\text{ch}}^2}\right. \right.\right.$$
$$\left.\left.\left. + 4\frac{D\tau_{\text{tx/rx}}}{u_{\text{tx/rx}}^2}(\alpha_{\text{ch}}^{(11)})^2 \alpha_{\text{tx/rx}}^2\right)4\pi^2 \frac{1}{T_0^2}\right)\right). \tag{42}$$

VI. Conclusion

In this paper, the interference modeling and capacity analysis for the microfluidic MC channel are presented. The impact of interferer signal on the MC capacity is studied for single and multiple interferer cases. The MC capacity is shown to be severely limited under interference, which requires development of practical interference-aware communication schemes considering the capabilities of the biological molecular transmitters and receivers. Furthermore, three different MIC configurations are introduced based on the flow velocity and the receiver placement on the microfluidic channel, namely, the microfluidic both-sided interference configuration, the microfluidic one-sided interference configuration, and the microfluidic interference-free configuration.

MC over microfluidic channels can enable in parallel sensing and processing of chemicals by molecular transmitters, and these transmitters can engage in multi-stage chemical reactions with the receivers via sending their message molecules over a common microfluidic channel. The modeling of the molecular transmitter and receivers is still an open research problem which can help to design a complete microfluidic MC system. To distinguish the designated signal from interference, the development of modulation and detection schemes based on constraints of biological transmitters and receivers, respectively, is essential.

References

[1] G. M. Whitesides, "The origins and the future of microfluidics," *Nature*, vol. 442, no. 7101, pp. 368–373, Jul. 2006.

[2] T. Vilkner, D. Janasek, and A. Manz, "Micro total analysis systems. Latest advancements and trends," *Anal. Chem.*, vol. 78, no. 12, pp. 3887–3907, Jun. 15, 2006.

[3] T. M. Squires and S. R. Quake, "Microfluidics: Fluid physics at the nanoliter scale," *Rev. Mod. Phys.*, vol. 77, no. 3, pp. 977–1026, Oct. 2005.

[4] D. Mark, S. Haeberle, G. Roth, F. von Stetten, and R. Zengerle, "Microfluidic lab-on-a-chip platforms: Requirements, characteristics and applications," *Chem. Soc. Rev.*, vol. 39, pp. 1153–1182, 2010.

[5] D. Janasek, J. Franzke, and A. Manz, "Scaling and the design of miniaturized chemical-analysis systems," *Nature*, vol. 442, pp. 374–380, Jul. 27, 2006.

[6] T. Thorsen, S. J. Maerkl, and S. R. Quake, "Microfluidic large-scale integration," *Science*, vol. 298, no. 5593, pp. 580–584, Oct. 18, 2002.

[7] H. A. Stone, A. D. Stroock, and A. Ajdari, "Engineering flows in small devices: Microfluidics toward a lab-on-a-chip," *Ann. Rev. Fluid Mechan.*, vol. 36, pp. 381–411, Jan. 2004.

[8] J. Melin, and S. R. Quake, "Microfluidic large-scale integration: The evolution of design rules for biological automation," *Ann. Rev. Biophys. Biomol. Struct.*, vol. 36, pp. 213–231, Jun. 2007.

[9] I. F. Akyildiz, J. M. Jornet, and M. Pierobon, "Nanonetworks: A new frontier in communications," *Commun. ACM*, vol. 54, no. 11, pp. 84–89, Nov. 2011.

[10] I. F. Akyildiz, F. Brunetti, and C. Blazquez, "Nanonetworks: A new communication paradigm," *Comput. Netw. J. (Elsevier)*, vol. 52, no. 12, pp. 2260–2279, Aug. 2008.

[11] P. J. Lee, P. J. Hung, V. M. Rao, L. P. Lee "Nanoliter scale microbioreactor array for quantitative cell biology," *Biotechnol. Bioeng.*, vol. 94, no. 1, May 5, 2006.

[12] T. Danino, O. Mondragon-Palomino, L. Tsimring, and J. Hasty, "A synchronized quorum of genetic clocks," *Nature*, vol. 463, no. 7279, pp. 326–330, Jan. 2010.

[13] B. M. Willardson, J. F. Wilkins, T. A. Rand, J. M. Schupp, K. K. Hill, P. Keim, and P. J. Jackson, "Development and testing of a bacterial biosensor for toluene-based environmental contaminants," *Appl. Environ. Microbiol.*, vol. 64, no. 3, pp. 1006–1012, Mar. 1998.

[14] S. Leth, S. Maltoni, R. Simkus, B. Mattiasson, P. Corbisier, I. Klimant, O. S. Wolfbeis, and E. Csoregi, "Engineered bacteria based biosensors for monitoring bioavailable heavy metals," *Electroanalysis*, vol. 14, no. 1, pp. 35–42, Jan. 2002.

[15] T. Elad, J. H. Lee, M. B. Gu, and S. Belkin "Microbial cell arrays," *Adv. Biochem. Eng./Biotechnol.*, vol. 117, pp. 85–108, 2010.

[16] S. Daunert, G. Barrett, J. S. Feliciano, R. S. Shetty, S. Shrestha, and W. Smith-Spencer, "Genetically engineered whole-cell sensing systems: Coupling biological recognition with reporter genes," *Chem. Rev.* vol. 100, no. 7, pp. 2705–2738, Jul. 2000.

[17] S. Belkin, "Microbial whole-cell sensing systems of environmental pollutants," *Curr. Opinion Microbiol.*, vol. 6, no. 3, pp. 206–212, Jun. 2003.

[18] S. Magrisso, Y. Erel, and S. Belkin, "Microbial reporters of metal bioavailability," *Microbial Biotechnol.*, vol. 1, no. 4, pp. 320–330, 2008.

[19] S. J. Sorensen, M. Burmolle, and L. H. Hansen, "Making bio-sense of toxicity: New developments in whole-cell biosensors," *Current Opinion Biotechnol.*, vol. 17, vol. 1, pp. 11–16, Feb. 2006.

[20] I. F. Akyildiz, F. Fekri, R. Sivakumar, C. R. Forest, and B. K. Hammer, "MONACO: Fundamentals of molecular nano-communication networks," *IEEE Wireless Commun.*, vol. 19, no. 5, pp. 12–18, Oct. 2012.

[21] B. Krishnaswamy, C. M. Austin, J. P. Bardill, D. Russakow, G. L. Holst, B. K. Hammer, C. R. Forest, and R. Sivakumar, "Time-elapse communication: Bacterial communication on a microfluidic chip," *IEEE Trans. Commun.*, vol. 61, no. 12, pp. 5139–5151, Dec. 2013.

[22] C. M. Austin, W. Stoy, P. Su, M. C. Harber, J. P. Bardill, B. K. Hammer, and C. R. Forest, "Modeling and validation of autoinducer-mediated bacterial gene expression in microfluidic environments," *Biomicrofluidics*, vol. 8, no. 3, art. no. 034116, 2014.

[23] B. D. Unluturk, A. O. Bicen, and I. F. Akyildiz, "Genetically engineered bacteria-based biotransceivers for molecular communication," to appear in *IEEE Trans. Commun.*, 2015.

[24] M. Pierobon and I. F. Akyildiz, "Capacity of a diffusion-based molecular communication system with channel memory and molecular noise," *IEEE Trans. Inform. Theory*, vol. 59, no. 2, pp. 942–954, Feb. 2013.

[25] B. Atakan and O. B. Akan, "Deterministic capacity of information flow in molecular nanonetworks," *Nano Commun. Netw.*, vol. 1, no. 1, pp. 31–42, Mar. 2010.

[26] M.T. Barros, S. Balasubramaniam, B. Jennings, and Y. Koucheryavy, "Transmission protocols for calcium-signaling-based molecular communications in deformable cellular tissue," *IEEE Trans. Nanotechnol.*, vol. 13, no. 4, pp. 779–788, Jul. 2014.

[27] D. Kilinc and O. B. Akan, "An information theoretical analysis of nanoscale molecular gap junction communication channel between cardiomyocytes," *IEEE Trans. Nanotechnol.*, vol. 12, no. 2, pp. 129–136, Mar. 2013.

[28] M. Pierobon and I. F. Akyildiz, "A statistical-physical model of interference in diffusion-based molecular nanonetworks," *IEEE Trans. Commun.*, vol. 62, no. 6, pp. 2085–2095, Jun. 2014.

[29] A. O. Bicen and I. F. Akyildiz, "System-theoretic analysis and least-squares design of microfluidic channels for flow-induced molecular communication," *IEEE Trans. Signal Process.*, vol. 61, no. 20, pp. 5000–5013, Oct. 2013.

[30] A. O. Bicen and I. F. Akyildiz, "End-to-end propagation noise and memory analysis for molecular communication over microfluidic channels," *IEEE Trans. Commun.*, vol. 62, no. 7, pp. 2432–2443, Jul. 2014.

[31] B. Kirby, *Micro- and Nanoscale Fluid Mechanics: Transport in Microfluidic Devices*. New York, NY, USA: Cambridge Univ. Press, 2010.

[32] H. Bruus, *Theoretical Microfluidics,*. London, U.K.: Oxford Univ. Press, 2008.

[33] K. W. Oh, K. Lee, B. Ahn, and E. P. Furlani, "Design of pressure-driven microfluidic networks using electric circuit analogy," *Lab Chip*, vol. 12, no. 3, pp 515–545, 2012.

[34] Y. Zhou, Y. Wang, T. Mukherjee, and Q. Lin "Generation of complex concentration profiles by partial diffusive mixing in multi-stream laminar flow," *Lab Chip*, vol. 9, no. 10, pp. 1439–1448, 2009.

[35] S. K. Griffiths and R. H. Nilson, "Design and analysis of folded channels for chip-based separations," *Anal. Chem.* vol. 74, no. 13, pp. 2960–2967, Jul. 2002.

[36] S. K. Griffiths and R. H. Nilson, "Low-dispersion turns and junctions for microchannel systems," *Anal. Chem.* vol. 73, no. 2, pp. 272–278, Jan. 2001.

[37] Y. Wang, T. Mukherjee, and Q. Lin, "Systematic modeling of microfluidic concentration gradient generators," *J. Micromech. Microeng.*, vol. 8, no. 5, pp. 2128–2137, Sep. 2006.

[38] D. Dutta and D. T. Leighton, "Dispersion reduction in pressure-driven flow through microetched channels," *Anal. Chem.*, vol. 73, no. 3, pp. 504–513, Feb. 2001.

[39] T. M. Cover and J. A. Thomas, *Elements of Information Theory*. New York, NY, USA: Wiley-Interscience, 2006.

A. Ozan Bicen (S'08) received the B.Sc. and M.Sc. degrees in electrical and electronics engineering from Middle East Technical University, Ankara, Turkey, in 2010 and from Koc University, Istanbul, Turkey, in 2012, respectively. He is currently working toward the Ph.D. degree at the School of Electrical and Computer Engineering, Georgia Institute of Technology, Atlanta, GA, USA, and is also a Graduate Research Assistant at the Broadband Wireless Networking Laboratory. His current research interests include molecular communication and nanonetworks.

Ian F. Akyildiz (M'86–SM'89–F'96) received the B.S., M.S., and Ph.D. degrees in computer engineering from the University of Erlangen-Nurnberg, Erlangen, Germany, in 1978, 1981, and 1984, respectively. He is currently the Ken Byers Chair Professor in Telecommunications with the School of Electrical and Computer Engineering, Georgia Institute of Technology, Atlanta, GA, USA, the Director of the Broadband Wireless Networking Laboratory, and the Chair of the Telecommunication Group at Georgia Tech. He is an honorary Professor with the School of Electrical Engineering at Universitat Politecnica de Catalunya, Barcelona, Spain, and founded the NaNoNetworking Center in Catalunya. He is also an honorary Professor with the Department of Electrical, Electronic, and Computer Engineering at the University of Pretoria, South Africa, and the Founder of the Advanced Sensor Networks Lab. Since September 2012, he is a Finland Distinguished Professor Program Professor, supported by the Academy of Finland, Department of Communications Engineering, Tampere University of Technology, Finland. His current research interests include nanonetworks, long-term evolution advanced networks, cognitive radio networks, and wireless sensor networks. He is the Editor-in-Chief of the *Computer Networks* (Elsevier) Journal, and the founding Editor-in-Chief of the *Ad Hoc Networks* (Elsevier) Journal, the *Physical Communication* (Elsevier) Journal, and the *Nano Communication Networks* (Elsevier) Journal. He is an ACM Fellow since 1997. He received numerous awards from the IEEE and the ACM.